



## Inherentness of Non-stationarity in Solar Wind

Vamsee Krishna Jagarlamudi, Thierry Dudok de Wit, Vladimir Krasnoselskikh, Milan Maksimovic

### ► To cite this version:

Vamsee Krishna Jagarlamudi, Thierry Dudok de Wit, Vladimir Krasnoselskikh, Milan Maksimovic. Inherentness of Non-stationarity in Solar Wind. The Astrophysical Journal, 2019, 871 (1), pp.68. 10.3847/1538-4357/aaef2e . hal-02408247

**HAL Id: hal-02408247**

**<https://hal.science/hal-02408247>**

Submitted on 24 Jan 2020

**HAL** is a multi-disciplinary open access archive for the deposit and dissemination of scientific research documents, whether they are published or not. The documents may come from teaching and research institutions in France or abroad, or from public or private research centers.

L'archive ouverte pluridisciplinaire **HAL**, est destinée au dépôt et à la diffusion de documents scientifiques de niveau recherche, publiés ou non, émanant des établissements d'enseignement et de recherche français ou étrangers, des laboratoires publics ou privés.



# Inherentness of Non-stationarity in Solar Wind

Vamsee Krishna Jagarlamudi<sup>1</sup> , Thierry Dudok de Wit<sup>1</sup> , Vladimir Krasnoselskikh<sup>1</sup> , and Milan Maksimovic<sup>2</sup>

<sup>1</sup>LPC2E, CNRS, University of Orléans, 3 Avenue de la Recherche Scientifique, F-45071 Orleans Cedex 2, France

<sup>2</sup>LESIA, Observatoire de Paris, 61 Avenue de l'Observatoire, F-75014 Paris, France

Received 2018 August 29; revised 2018 October 29; accepted 2018 November 5; published 2019 January 22

## Abstract

Most studies of turbulence in the solar wind invoke stationarity as a working hypothesis. Unfortunately, this concept is difficult to verify in practice. To investigate the validity of the weak stationarity assumption we consider magnetic field measurements made by the *WIND* satellite and study the properties of the autocorrelation function (ACF), which is a classical gauge for characteristic times or scales. We find that the ACF suffers from a high variance, which precludes the routine interpretation of correlation times and scales. In addition, the ACF fails to converge toward a constant function, even when considering the longest available intervals of either fast or slow solar wind. The reasons behind this lack of convergence are better understood by considering the power spectral density (PSD) of the magnetic field and analyzing synthetic data that exhibit the same PSD. Interestingly, we find evidence for an  $f^{-1}$  scaling at low frequencies in both fast and slow solar winds. These results, together with the theoretical properties of processes with  $f^{-\gamma}$  scaling all point to the non-stationary behavior of the solar wind, in particular for scales that correspond to the inertial range. They also impose strong constraints on the applicability of ACF analysis as a tool for characterizing statistical properties of solar wind turbulence.

**Key words:** magnetic fields – solar wind – turbulence

## 1. Introduction

The solar wind is an exceptional natural laboratory for performing in situ studies of astrophysical plasma turbulence (Bruno & Carbone 2013). A central issue and frequent underlying assumption in most of these studies is the stationarity of the solar wind. Stationarity implies strict invariance of statistical properties under all and every time shift (Beran 1994). This assumption is of paramount importance for properly characterizing finite amounts of noisy observations since it leads to many simplifications (Bendat & Piersol 2000). By raising the question of stationarity in the context of the solar wind our objective is not just to determine whether the wind is stationary or not (we shall see later that this is actually an ill-posed question) but rather to understand how departures from stationarity may affect our physical interpretation of the solar wind.

Although stationarity is often invoked as a working hypothesis in solar wind studies, several causes may potentially lead to its violation. Most are deeply rooted in the underlying physics. They include self-similarity and fractal properties of the turbulent cascade that involves a multiplicative process (Marsch & Tu 1997; Veltri 1999), the presence of coherent or organized structures such as shocks (Tu & Marsch 1995; Matthaeus et al. 2015), heavy-tailed distributions that may result, for example, from self-organized critical processes (Aschwanden et al. 2016), and the long-range memory associated with the sources of the solar wind (Nicol et al. 2009). Importantly, the corona, which is the source of the solar wind is always evolving in time and space, and can be the cause of non-stationarity. There may also be instrumental causes, such as the presence of discontinuities or drifting instruments (Rust et al. 2008).

There are several reasons for which the question of stationarity of the solar wind matters. First, stationarity is an essential but often implicit assumption behind most of the spectral and statistical analysis techniques that are routinely

used in solar wind studies: correlation functions and all quantities involving moments, the Fourier transform, linear filters, etc. When this assumption does not hold, many familiar mathematical results fail to hold and classical techniques may give results that are biased if not outright wrong. This bias comes with non-intuitive properties that can be very misleading as they often require unrealistically large samples to be properly identified and corrected (Witt et al. 1998; Franzke et al. 2012). Second, deviations from stationarity have recently been regarded by some as an untapped source of potential predictability and may thus serve for risk assessment and forecasting. A typical example is the presence of extreme events in the solar wind, which impact the Earth's magnetospheric dynamics (Moloney & Davidsen 2011).

Finally, there is the key question of whether non-stationarity is inherently part of the turbulent flow or if the solar wind may rather be considered as a stationary stochastic process with some large-scale structures that superimposed on it and thereby make it non-stationary. As we shall see, non-stationarity is inherently part of the solar wind in the timescales usually considered for turbulence studies.

Non-stationarity is traditionally illustrated with time series whose stochastic fluctuations are offset by some slow trend. This picture is too simplistic as non-stationarity can manifest itself in many other ways such as the volatility of short-scale fluctuations with a clustering of extreme values (Moloney & Davidsen 2014), and even in bounded binary signals. A considerable amount of work has been devoted to these different manifestations, which are intimately connected (e.g., Witt et al. 1998; Franzke et al. 2015) and may have significant implications on our physical understanding. Likewise, there are deep connections with long-range dependence, the Hurst exponent, and the presence of an  $f^{-1}$  scaling of the power spectral density (PSD) (Mandelbrot 1999; Gilmore et al. 2002; Graves et al. 2017). These are well beyond the scope of this study, in which we focus on the impact of non-stationarity on statistical studies of the solar wind.

Some authors have attempted to answer whether the solar wind is stationary or not. In their pioneering study, Matthaeus & Goldstein (1982b) concluded that statistical quantities such as the autocorrelation function (ACF) converge toward a constant value when considering intervals that are long enough, typically days to weeks. This would suggest that the solar wind is approximately stationary in time. Podesta & Roberts (2005) reached the same conclusion, with special emphasis on the validity of power spectral estimates. Perri & Balogh (2010) extended these results to different parameter ranges in the solar wind and concluded that in the inertial range of turbulence the assumption of stationarity only holds for fast and uniform solar wind flows.

These different studies suggest that the quest for the elusive stationarity of the solar wind remains largely unsolved. Such a quest should logically start with a succinct and realistic definition of what stationarity means. Alas, the definition of stationarity, which we mentioned earlier is a mathematical concept that applies to populations but is inapplicable to real data with finite samples. For that reason, most studies concentrate on weak-sense (wide-sense or second-order) stationarity, which requires the first- and second-order moments only to be time invariant rather than all of them (Priestley 1988). That is, the expected mean  $\mathbb{E}[x(t)] = m_x(t)$  and variance  $\mathbb{E}[(x(t) - m_x(t))^2] = \sigma_x^2(t)$  on any time interval should both be independent of time, where  $\mathbb{E}(\cdot)$  stands for the expectation. In addition, the autocovariance function

$$C(t, \tau) = \mathbb{E}[(x(t) - m_x(t))(x(t + \tau) - m_x(t + \tau))], \quad (1)$$

should only depend on the time difference  $\tau$ , so that  $C(t, \tau) = C(\tau)$ . Equivalently, the ACF,

$$\text{ACF}(t, \tau) = \frac{C(t, \tau)}{C(t, 0)}, \quad (2)$$

should also be time-independent, i.e.,  $\text{ACF}(t, \tau) = \text{ACF}(\tau)$ .

As Bendat & Piersol (2000) pointed out, these criteria apply to mathematical expectations (i.e., probability-weighted averages) and make sense when instantaneous time averages can be performed, which cannot be realistically done when working with finite samples that consist of time series from single-spacecraft observations. Our problem then consists in determining whether the statistical properties that are estimated from finite time intervals do not *significantly* vary in time.

Multiple approaches have been developed for that purpose, (e.g., Priestley & Rao 1969; Bendat & Piersol 2000; Borgnat & Flandrin 2009). This is an active field of research that has received more attention in geophysics and econometrics than in space sciences, presumably because of its direct economic impacts. Among these different approaches, the ACF offers several advantages and has been widely used. First, its expression directly appears in the definition of weak stationarity. Second, it allows us to check how the integral scales are affected by the absence of stationarity.

Considerable attention has been paid in solar wind studies to the estimation of characteristic scales (Bruno & Carbone 2013) from the ACF. Among these there is the integral scale (sometimes called correlation length), which is the largest spatial scale of the inertial range (Batchelor 1953). The integral scale is related to the size of the largest energy-containing eddies (Matthaeus et al. 1998; Alexandrova et al. 2013). The ACF generally decays monotonically and its decay time then provides an estimate of the largest eddy. Its study is partly

motivated by the constraints in its evolution throughout the heliosphere may pose on turbulence models (see Bruno & Carbone 2013, and references therein). In the solar wind, fluctuating fields are generally advected past the spacecraft in a shorter time than their characteristic dynamical timescale. Importantly in the inertial range, where magnetic field fluctuations dynamically evolve at the Alfvén speed ( $V_A \approx 50 \text{ km s}^{-1}$ ), while the flow propagates at about  $V_{\text{flow}} \approx 400\text{--}500 \text{ km s}^{-1}$ ; therefore, it is customary to invoke Taylor’s frozen-in hypothesis and interpret these spatial scales as durations in the observed time series. Unfortunately, since the ACF is sensitive to non-stationarity, the outcome of the above approaches has to be tested for the effect of non-stationarity.

Many authors have investigated ACFs in the solar wind: Klein et al. (1992), Tu & Marsch (1995), Richardson & Paularena (2001), King & Papitashvili (2005), Matthaeus et al. (2005), Podesta et al. (2008), Wicks et al. (2010), and Marquette et al. (2018) to cite a few. However, most of them did not question the effect of non-stationarity on the studied ACFs, which will precisely be our focus here. There are also more practical reasons for working with ACFs: solar wind observations are often plagued by data gaps. It is then easier to work with the ACF, which can be easily estimated from incomplete data (Scargle 1989) rather than with Fourier or wavelet transforms. In what follows, we shall concentrate on the ACF only and investigate what new insight it gives us into the presence of non-stationarity at different timescales and in different regimes of the solar wind.

Let us finally mention that various statistical tests have been designed for testing the hypothesis of non-stationarity. The augmented Dickey–Fuller test (Dickey & Fuller 1979) is one among them. Here, we deliberately focus on the ACF because of its physical interpretation and its strong connection to the concept of second-order stationarity.

This article is structured as follows. In Section 2, we present the solar wind data. Section 3 addresses the results. First we present the ACF results before considering the PSD and connecting it to theoretical expressions of the ACF. These are then compared with synthetic data sets. These results are then discussed in Section 4, which is followed by the conclusions in Section 5.

## 2. Solar Wind Data

In the following we consider magnetic field observations made between 2006 and 2016 by the fluxgate magnetometer (Lepping et al. 1995) onboard the *WIND* satellite. *WIND* offers long (>2 days) and uninterrupted records of the solar wind in fast and slow solar wind regimes, which allows us to collect large samples from each regime. The time resolution of these records is 15 s, so we can investigate stationarity on timescales that range from seconds to days. The range includes the integral scale, which is typically 1–2 hr, and covers most of the inertial range. During that period, *WIND* was positioned in halo orbit around the L1 Lagrange point, constantly observing the Sun from the ecliptic plane, at a constant distance of 1 au from the Sun.

In Figure 1 we illustrate two excerpts taken from the fast and slow solar wind. Both reveal strong fluctuations at all scales, which some might already consider as signatures of non-stationarity.

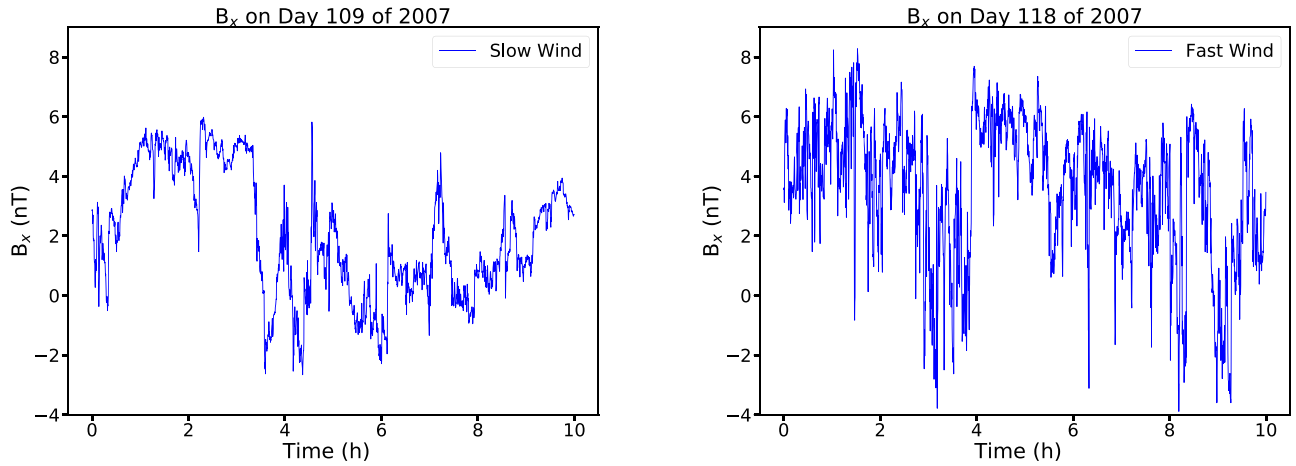


**Figure 1.** Illustration of 10 hr of radial magnetic field observations made in 2007, in the slow wind (left plot) and in the fast wind (right plot).

Since the origin and the properties of the two regimes of the solar wind differ, it is important to analyze the statistical properties separately, similarly to what Perri & Balogh (2010) did. The periods during which *WIND* observes pure fast solar wind were at best a few days long, which sets the upper limit of the timescales we can reasonably inspect.

In what follows, fast winds are defined by  $v > 600 \text{ km s}^{-1}$  and slow winds by  $v < 400 \text{ km s}^{-1}$ . The three components of the magnetic field are known to give qualitatively similar results (e.g., Wicks et al. 2010), so we concentrate on the radial component  $B_x$  only. The physically relevant quantities are spatial scales, not their duration. However, since the ACF is estimated in the time domain, we shall concentrate on temporal scales only. Using Taylor’s “frozen-in” hypothesis we can convert times into lengths simply by multiplying them by the mean flow velocity. The interpretation of spatial scales will further be addressed in Section 4.

### 3. Results

#### 3.1. ACF Analysis

The formal expression of the ACF (Equations (1) and (2)) that enters the definition of weak stationarity applies for populations only. Therefore, we cannot directly apply them to finite samples. First, we need to replace expectations by sample averages (Bendat & Piersol 2000; Papoulis & Pillai 2002)

$$\text{ACF}(t, \tau) = \frac{\langle (x(t) - m_x)(x(t + \tau) - m_x) \rangle_T}{\sigma_x^2} \quad (3)$$

where  $x(t)$  is the magnetic field,  $\langle \dots \rangle$  stands for sample averaging over a sample of size  $T$ , and  $m_x$  and  $\sigma_x^2$  are respectively the sample mean and the sample variance.

Second, since our observations are discrete functions of time and not continuous ones, integrals need to be replaced by sums. Although these two differences are routinely encountered in data analysis, in the particular context of non-stationarity the distinction between populations and finite samples is far from trivial and has far-ranging consequences (see, for example, Kasdin 1995). In particular, the duration  $T$  (or sample size) comes in as an additional parameter and one needs to distinguish what part of the observed ACF reflects the properties of the sample and what part is influenced by the choice of the estimator. That is, the estimation and the detection problems are now intimately connected.

Surprisingly, this issue, which is central to the identification of non-stationarity, is rarely addressed explicitly in the literature. As Bendat & Piersol (2000) point out, the only workaround is to relax the initial definition of weak stationarity and consider a weaker version of it that consists in determining whether the mean and ACF significantly vary from one time interval to the other. Since there is no reference value here to determine what we call significant, it immediately appears why the formulation of a rigorous statistical test is so difficult.

Let us therefore follow a more exploratory approach and investigate how the ACF of the solar wind varies with occurrence time  $t$  and sample size  $T$ .

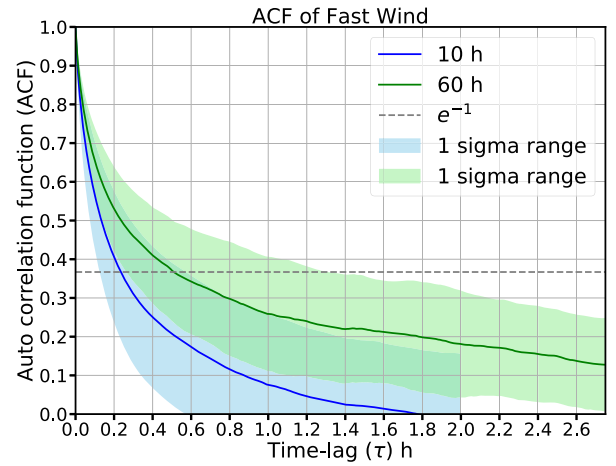
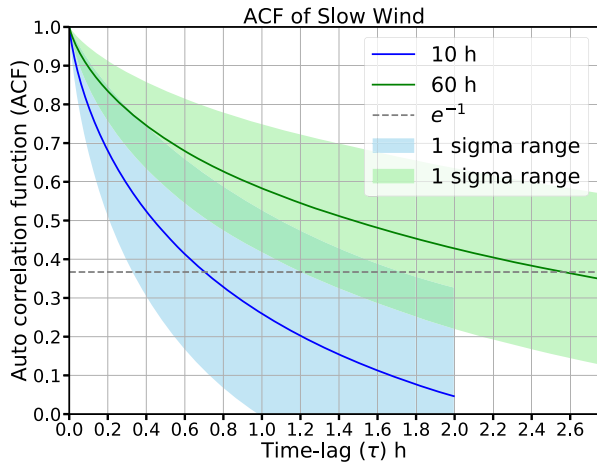
The integral timescale of solar wind turbulence is typically thought to be around 1–2 hr, so we need to observe the solar wind for at least 10 hr to be able to properly estimate the ACF for different lags. We selected non-overlapping intervals of various lengths and estimated the ACF for each of them. In the fast solar wind we found respectively 420, 163, 51, and 23 intervals with 10, 20, 40, and 60 hr of pure fast wind. In the slow solar wind we found, respectively, 4409, 2026, 875, and 508 intervals. *WIND* spends more time in the slow wind because it is located in the equatorial plane. For durations longer than 60 hr the number of occurrences drops rapidly and with it the statistical quality of estimated ACF.

Figure 2 displays the average ACF obtained for both solar wind regimes for samples of 10 and 60 hr duration only. The largest lag we explore is set at  $T/5$  to prevent the variance of the ACF from becoming excessively large (Press et al. 2002). Also shown is the standard deviation of the ACF, which quantifies the dispersion of the values. All ACFs decay quasi-monotonically to zero, which illustrates the gradual loss of information.

Two outstanding results are the large dispersion of the ACFs, which implies that its values varies considerably from one sample to another, and the major difference observed between ACFs estimated from intervals lasting for 10 and 60 hr. Both results raise serious concerns about the physical interpretation of these results.

Many simple solar wind models approximate the solar wind as a stochastic first-order Markov process whose future state solely depends on the present state and not on the past history. Markov processes (more specifically, Ornstein–Uhlenbeck processes) are characterized by an ACF that decays





**Figure 2.** ACF of slow and fast solar wind along with their dispersion, which is expressed by  $\pm 1$  standard deviation.

exponentially (Papoulis & Pillai 2002)

$$\text{ACF}(\tau) = \frac{C(\tau)}{C(0)} = e^{-|\tau|/t_c}. \quad (4)$$

The correlation time ( $t_c$ ) is usually estimated by means of the  $e$ -folding technique by considering the time it takes for the ACF to drop to  $e^{-1}$  of its maximum value (Matthaeus et al. 1998; Weygand et al. 2013; Ruiz et al. 2014). A more general definition of the memory or correlation scale is (Frisch 1995)

$$t_c = \int_0^\infty \frac{C(\tau)}{C(0)} d\tau. \quad (5)$$

For Markov processes this definition of  $t_c$  coincides with the one from Equation (4). In practice, ACFs rarely show a pure exponential decay, and therefore the estimator based on Equation (4) is approximate. However, in spite of these limitations, the  $e$ -folding estimator is widely considered and we shall use it for the mere sake of continuity.

In Figure 2 the  $e$ -folding time is given by the intersection between the ACF and the horizontal dashed line. We find the correlation time to be longer in the slow than in the fast solar wind with a value that is of the order of 1–2 hr. These properties have already been documented by several authors (Weygand et al. 2013; Isaacs et al. 2015). Because of the large dispersion in the ACFs there is a large dispersion as well in the correlation time  $t_c$ . This is illustrated in Figure 3 by the histogram of  $t_c$ , which is calculated using the  $e$ -folding method for 10 hr samples of the fast wind. Such a large dispersion may be caused either by a lack of stationarity or by the poor convergence of our estimator of the ACF (Equation (3)), or by both. At this stage we cannot tell yet.

To further investigate how the duration  $T$  affects the ACF, we plot in Figure 4 the ACF for the two solar wind regimes with  $T = 10, 20, 40$ , and 60 hr. A striking result is the continuous change in the ACF with sample duration with no apparent evidence for convergence. This behavior is in contradiction with standard belief, since one would normally expect the ACF to converge toward a fixed function when the sample length becomes much longer than the correlation time. Here, even with 60 hr of observations we see no evidence for convergence.

Isaacs et al. (2015) in their statistical study observed a similar lack of saturation; the reason they suggested was the

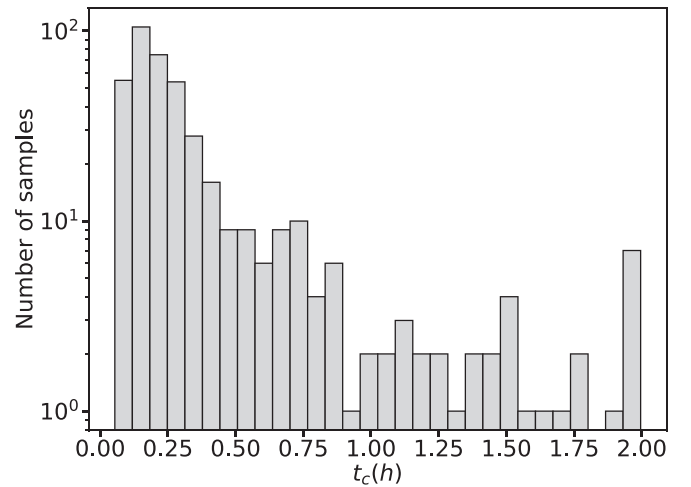


**Figure 3.** Histogram of the correlation time  $t_c$  estimated from 420 intervals of 10 hr each using the  $e$ -folding method, in the fast solar wind.

presence of long-range correlated structures. They suggested to select a proper sample size of the order of 10–20 hr to avoid that effect. This, however, goes against one of the major assumptions of stationarity, which is the invariance versus translation in time.

One might argue that intervals of 60 hr are still too short to properly estimate the ACF. For that reason we extended the analysis to intervals of 300 hr, but in the slow solar wind only, see Figure 5. This figure shows no evidence for convergence either. There is a frequent belief that longer records (lasting for weeks to years) should eventually yield better estimates of the ACF and a pertinent basis for investigating non-stationarity. Matthaeus & Goldstein (1982b), for example, considered a long sample of 2 years. However, unless the satellite is co-rotating with the Sun, the observations of the solar wind will be modulated by solar rotation and therefore be approximately cyclostationary (Gardner et al. 2006), with a period of about 27 days. This property excludes the proper assessment of non-stationarity in solar wind records that exceed a few days. In addition, since the fast and slow winds have different properties the ACF of their mixture will be polluted by transitions between these two regimes. Recently, Franzke et al. (2015) have even shown that in some cases the switching between different regimes may precisely be the cause for non-stationarity

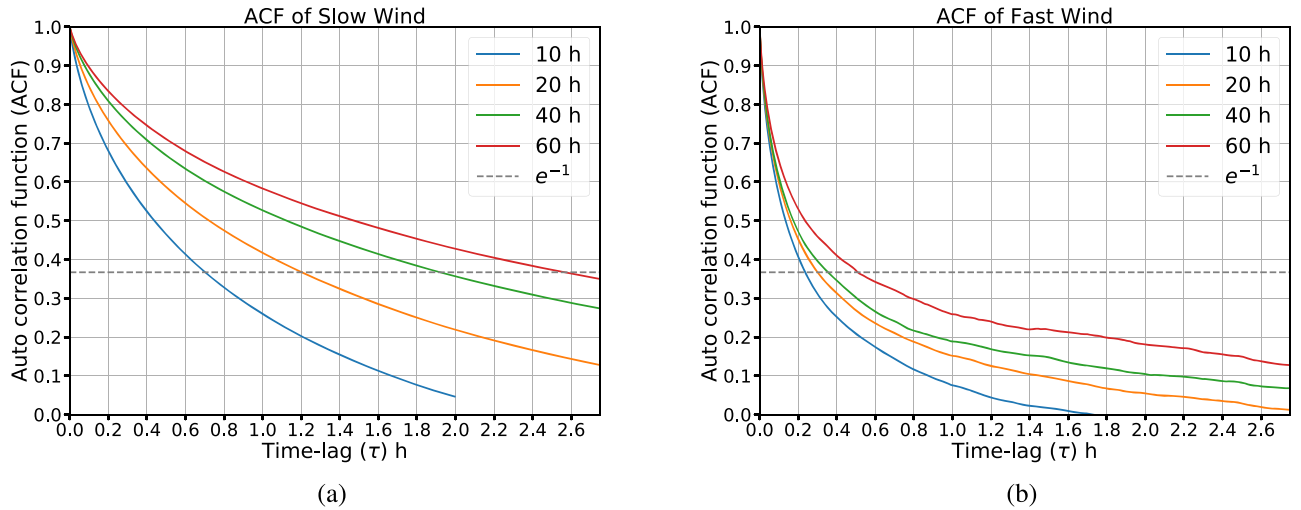


**Figure 4.** ACF of the  $B_x$  component at 1 au for different sample durations of 10, 20, 40, and 60 hr for slow winds only (a) and for fast winds only (b). The dashed horizontal line represents the  $e^{-1}$  value.

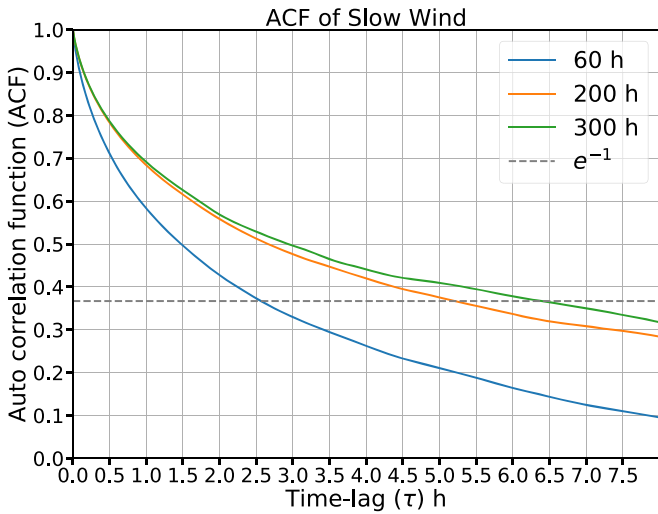


**Figure 5.** Same as Figure 4 but for longer samples of the solar wind of up to 300 hr.

and long-range dependence rather than the intrinsic properties of individual regimes.

At this stage, we conclude that the ACF of the solar wind cannot be meaningfully estimated for fast or slow solar winds, even with the longest available time intervals during which the solar wind remains in one single regime. This disconcerting result questions the physical meaning of correlation times that are routinely inferred from the solar wind. The smooth shape of ACFs that are estimated from individual samples is particularly misleading since it gives the false impression of a small uncertainty, which is definitely not the case.

To better understand the origin of these properties and their connection to stationarity let us now express the properties of the radial magnetic field in Fourier space and estimate for that purpose the PSD.

### 3.2. Power-law Scaling of the PSD

The PSD and the ACF are intimately related through the Wiener–Khinchin theorem, which states that the PSD is the Fourier transform of the ACF. The two provide complementary

(but not strictly equivalent) approaches for identifying characteristic scales (Ghil et al. 2002) and the equivalence between power laws in the PSD and in the ACF can be extended to non-stationary processes (Flandrin 1989). Here, we consider the PSD to better understand how the characteristic scales of the magnetic field are related to stationarity properties. As before, we concentrate on the radial component  $B_x$ .

To estimate the PSD, we consider Welch’s periodogram method and divide records into  $N$  different segments that overlap by 50%, apply to each of them a Hanning window, compute their Fourier transform, and average the squared magnitude of the latter. We consider the same samples as for the estimation of the ACF. Occasional small data gaps are linearly interpolated. Munteanu et al. (2016) have shown that it is a reasonable approach for estimating the PSD, except for the highest frequencies, which are not a matter of concern here.

The main result is a familiar double power law  $P(f) \propto f^{-\gamma}$  whose spectral index  $\gamma$  approaches 1 at low frequencies and is closer to 1.7 in the inertial range. Similar power laws have been observed by many in the solar wind (Bruno & Carbone 2013, and references therein) and their spectral indices have been abundantly discussed. Notice the presence of an  $f^{-1}$  scaling at low frequencies in both slow and fast wind regimes. Such scalings had been observed before in the fast wind (Bruno & Carbone 2013). As far as we know, however, this is the first evidence for an  $f^{-1}$  scaling in the slow wind.

The main message from Figure 6 is the presence of a double power law, which suggests that there is no characteristic scale in the magnetic field, except for the scale corresponding to the spectral break occurring between  $10^{-4}$  and  $10^{-3}$  Hz. This corresponds to a timescale of the order of 30 minutes to 3 hr, which is often interpreted as the integral scale. The main advantage of the PSD over the ACF is its lower sensitivity to non-stationarity, thanks to which the inferred scale lengths are less affected by the choice of the sample length (or rather, the window length when using Welch’s method). Comparable power-law scalings are observed for the two other components of the magnetic and for observables such as the wind velocity. Let us therefore relate this property of the PSD to the functional shape of the ACF.

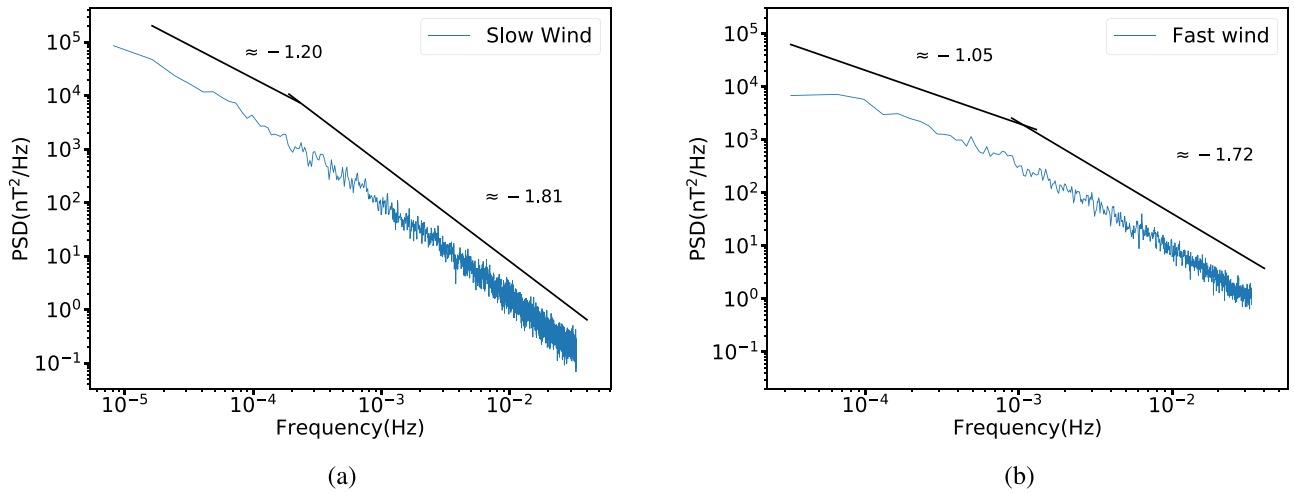


**Figure 6.** PSD of the  $B_x$  component, using *WIND* observations and the periodogram method. The left plot shows the slow wind and the right plot the fast wind. Lines corresponding to spectral indices ( $\gamma$ ) have been drawn to help locate different power laws.

### 3.3. Connecting the ACF to the PSD

Given the ubiquity of power-law scalings in the PSD of the solar wind, we now investigate how such a scaling affects the analytical expression of the ACF. Several authors have studied the analytical properties of the ACF of a time series whose PSD is a power law with spectral index  $\gamma$  (Hooge et al. 1981; Keshner 1982; Kasdin 1995; Hooge & Bobbert 1997). Following Kasdin (1995) we can show that if the ACF is calculated over a time interval occurring a long time  $t \gg \tau$  after the transients have vanished (which is a reasonable assumption for the solar wind), then the autocovariance can be approximated by: when  $0 < \gamma < 1$ ,

$$C(t, \tau) = C(\tau) \propto |\tau|^{\gamma-1}. \quad (6)$$

When  $\gamma = 1$ ,

$$C(t, \tau) \propto \log 4t - \log |\tau|. \quad (7)$$

When  $1 < \gamma < 2$ ,

$$C(t, \tau) \propto t^{\gamma-1} - c|\tau|^{\gamma-1}, \quad (8)$$

where  $c > 0$  is a constant. These asymptotic results apply to the autocovariance. To convert them into autocorrelations we normalize them by  $C(t, \tau = 0)$ . The key result is the presence of an offset depending on  $t$  that may be arbitrarily large when  $1 \leq \gamma \leq 2$ , i.e., for spectral indices that are routinely encountered in solar wind turbulence. More precisely, the characteristic scale we infer from the decay of the ACF is determined both by the underlying physics *and* by the observing window and in this sense also by sample length  $T$ .

This disconcerting result actually is a simple consequence of scale invariance in turbulence. Indeed, for a time series  $f(t)$  whose PSD has a power-law scaling with scaling index  $\gamma$ , we have  $f(\lambda t) \doteq \lambda^H f(t)$  where  $\doteq$  means that the two time series have the same finite joint distribution function for any  $H > 0$ . There is no such characteristic scale for  $f(t)$ , which is then called self-affine. Consequently, when we select an interval of duration  $T$  to estimate the  $e$ -folding time, the only timescale that stands out is the duration  $T$ .

These properties already point to the non-stationarity of the synthetic time series, which we will investigate below in more detail with a discussion on the impact of a double power law.

There is a second message in Equations (6)–(8). For most solar wind regimes, the ACF does not decay exponentially as for a first-order Markov process, but falls off more slowly with a power-law scaling. Such a behavior is well known to occur in systems that exhibit long-range correlations (Beran 1994). As a consequence, the  $e$ -folding time is not a proper estimator of the characteristic timescale. However, since the very concept of timescale breaks down anyway, and since most autocorrelations exhibit a monotonic decay, the  $e$ -folding time remains a crude but convenient means for quantifying the correlation time.

### 3.4. Synthetic Solar Wind Data: Single Power Law

To better illustrate the impact of self-affinity on the ACF we simulated synthetic magnetic field data whose PSD is a power law with a given spectral index. Let us first consider the case when the PSD consists of a single power law. The impact of double power laws will be addressed later.

To generate synthetic data we compute the Fourier transform of a sequence of white noise, apply the desired spectral index, and invert the Fourier transform (Kasdin 1995). The length of the sequences equals that of the solar wind records, namely, 14,400 samples for 60 hr of *WIND* data. With this approach, we generate 1000 records that mimic the properties of 10, 20, 40, and 60 hr of solar wind, while enabling us to carry out statistical tests. Our approach could be refined by imposing, for example, the magnetic field and the synthetic data to have the same probability distribution function, using the surrogate data technique (Theiler et al. 1992). However, since we are concerned with second-order moments only, there is no sound justification for tuning the probability density function, which is close to normal anyway.

Figure 7 summarizes the main results by displaying the average ACF for four different spectral indices:  $\gamma = 0.5, 1, 5/3$  (i.e., for a Kolmogorov model), and 3. For each case, 1000 synthetic time series were generated, and their individual ACFs averaged. A striking property of the ACFs is their dependence on the spectral index: the larger  $\gamma$  is, the slower the ACF decays, and the longer the memory of the system is. The main result for our purposes, however, is the difference between ACFs estimated from sequences of  $T = 10, 20, 40$ , and 60 hr. The figure confirms what had been observed with real magnetic

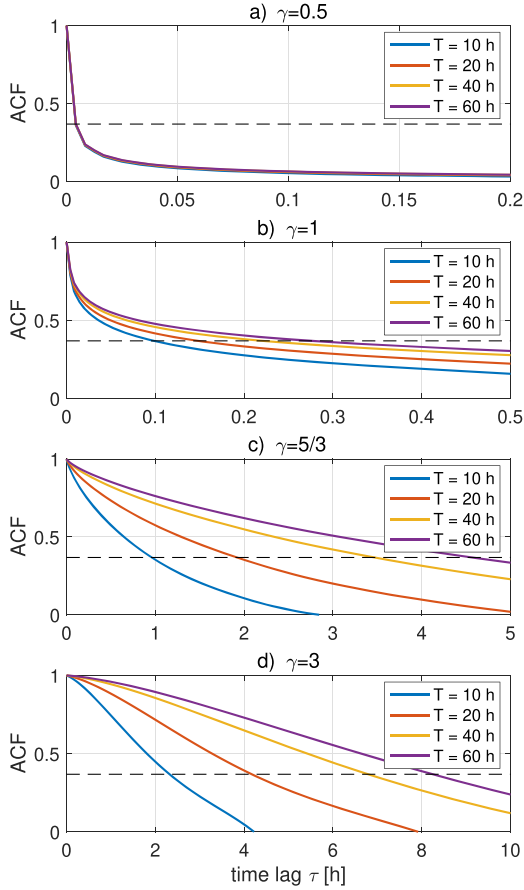


**Figure 7.** ACF of synthetic data for four spectral indices, from top to bottom:  $\gamma = 0.5$ ,  $\gamma = 1$ ,  $\gamma = 5/3$  (i.e., Kolmogorov model), and  $\gamma = 3$ . All plots show the average ACF for 1000 realizations that have the same length as the original data in Figure 4. The intersection with the horizontal dashed line defines the  $e$ -folding time.

field data, namely, that there is no apparent convergence to a fixed shape when increasing the length of the sequences. This lack of convergence is particularly evident for  $\gamma = 1$  and for  $\gamma = 5/3$ , in agreement with the analytical expressions given in Equations (6)–(8). The same holds for  $\gamma = 3$ , while on the contrary for  $\gamma = 0.5$  the ACFs seem to collapse on a fixed shape, regardless of the value of  $T$ .

Regarding the dispersion of the ACF we observe the same behavior as for the solar wind data in Section 3.1, namely, a large dispersion that precludes the precise determination of the ACF and its correlation time.

A natural approach to reducing the dispersion of the ACFs would be to estimate them from longer records. In a somewhat different context, Kiyani et al. (2009) investigated the weak stationarity by studying the exponents of the second-order structure functions of different physical processes. Their study concluded that if smaller sample sizes are used for the analysis, depending upon the process, the scaling exponent estimates are most likely dispersive due to the pseudo-non-stationarity. To test the method of reducing the dispersion of ACF using longer records we simulated an ensemble of 1000 self-affine records with a given spectral index  $\gamma$  and for each of them estimated the ACF by using intervals of duration  $T = 10, 20, 40$ , and  $60$  hr. We subsequently focus on the lag closest to the  $e$ -folding time and estimate the standard deviation  $\sigma_{\text{ACF}(t_e)}$  of the ACFs at that particular lag.

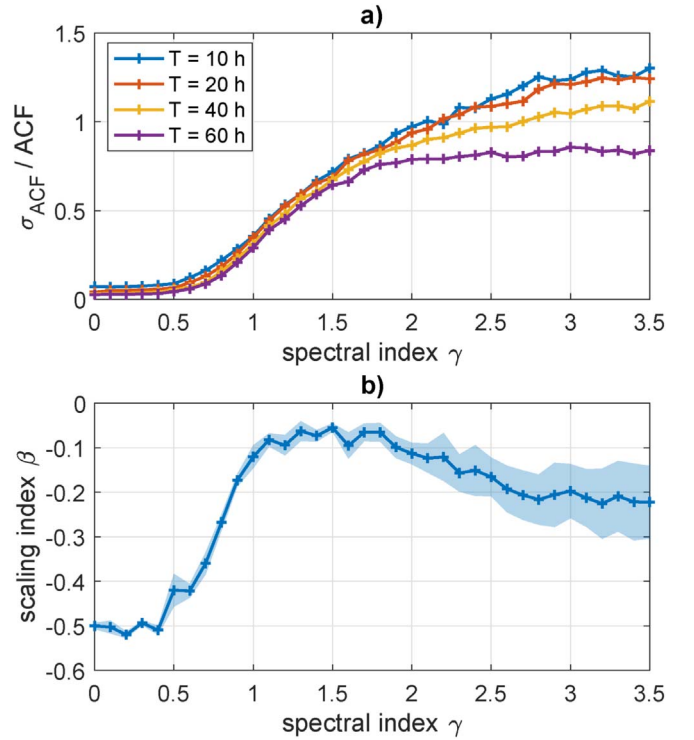


**Figure 8.** Upper plot: relative standard deviation of the ACF  $\sigma_{\text{ACF}(t_e)}/\text{ACF}(t_e)$ , measured at the  $e$ -folding time for simulated self-affine records with different values of the spectral index  $\gamma$ . Lower plot: scaling index  $\beta$  and its confidence interval ( $\pm$  one standard deviation), estimated from samples of duration  $T = 10, 20, 40$ , and  $60$  hr. An ensemble of 1000 realizations was used to estimate these quantities.

There are two major conclusions we can draw from these simulations, whose results are summarized in Figure 8. First, notice how the standard deviation of the ACFs gradually increases with the spectral index; its value really takes off when  $\gamma$  exceeds 1 and then keeps on increasing, eventually exceeding 100% when  $\gamma$  is greater than 2. This result already warns us about the high uncertainty of the ACF for steep power laws.

Such a high uncertainty would be acceptable if it could be reduced by further increasing  $T$ . Bartlett (1946), working under the assumption of stationarity, has shown that the standard deviation should approximately decrease as  $\sigma_{\text{ACF}} \propto T^{-1/2}$ . We consider instead the more generic scaling  $\sigma_{\text{ACF}} \propto T^\beta$  and investigate whether  $\beta$  can be closer to zero, which would imply a slower convergence and therefore be less favorable. Figure 8 indeed shows that the expected scaling with  $\beta = -1/2$  is observed only for small spectral indices with  $\gamma < 1$ . For steeper power laws  $\beta$  rapidly approaches zero, which means that much longer records are required to achieve the same reduction in uncertainty. This result vividly illustrates why self-affine processes with spectral indices above 1 are pathological and require extra care (Beran et al. 2016). Notice that while  $\beta$  slowly becomes more negative again when  $\gamma > 2$  the uncertainty still remains prohibitively large.

From this short inspection we conclude that the ACF of self-affine time series cumulates several pitfalls that can easily lead to fallacious interpretations of the correlation time. Unfortunately, most problems arise for spectral indices that fall between 1 and 2, which precisely coincides with the inertial range and  $f^{-1}$  range of solar wind turbulence.

Does it then mean that the ACF is worthless? Probably not because values obtained under identical conditions may still be



compared, taking into account their large uncertainty. While their absolute values are incorrect, they can still potentially be used for comparison purposes.

### 3.5. Synthetic Solar Wind Data: Double Power Law

So far we have concentrated on self-affine processes that exhibit one single power law in the PSD. Long observations of solar wind turbulence show that we have at least two power laws (Kiyani et al. 2015), followed by a steeper decay in the kinetic range. Here, we ignore the latter because most magnetic field observations (from fluxgate magnetometers) and wind velocity measurements cannot resolve its short timescales.

Extending Equations (6)–(8) to double power laws is not straightforward. Therefore, we generated synthetic time series whose PSD manifests a double power law with various spectral indices and break frequencies; the latter refers to the frequency at which the transition occurs between two spectral indices. Fortunately, the main results for such double power laws are a direct generalization of the single power-law case. They can be summarized by considering the two characteristic frequencies of the sample: the sampling frequency  $(\Delta t)^{-1}$  at the high end and the inverse duration  $T^{-1}$  at the low end:

1. If both characteristic frequencies belong to the frequency range in which a power law is observed with the same spectral index, then the results of the previous section apply (single power-law case).
2. If the two characteristic frequencies belong to ranges with different spectral indices, then the properties of the ACF are dominated by the spectral index at the lowest frequencies.

In practice the situation is not always clear cut, especially since the transition from one index to another is gradual. A robust result, however, is the strong impact of the low-frequency end of the PSD on the properties of the record.

Most solar wind studies rely on fluxgate magnetometer data or on velocity data whose highest frequency (sampling rate) is of the order of 1 Hz. These studies generally consider intervals of several hours at most. Their characteristic frequencies, the low-frequency value that is sample dependent and the high frequency value that is sampling rate-dependent belong to the inertial range of turbulence.

Therefore, a single power-law model often applies, with a spectral index of  $3/2$ – $5/3$ . Unfortunately, this is the worst case scenario as far as stationarity is concerned because the ACF has a high variance and converges very slowly toward the average.

For studies that consider longer time intervals, typically 1 day or more, a double power-law model may be more relevant since the  $f^{-1}$  scaling enters into play. While this case is somewhat more favorable than the previous one because of the lower variance of the ACF, convergence remains very slow. Not surprisingly, Mandelbrot (1999) called such  $f^{-1}$  processes wildly self-affine.

## 4. Discussion

Since the formal existence of weak stationarity in solar wind observations cannot be proven, the better question is whether we have enough evidence to draw conclusions. As mentioned before, the main practical signature of non-stationarity in the solar wind is a significant variation of the ACF. Our observations first reveal a striking lack of convergence of the

ACFs, whose mean value fails to stabilize when increasing the sample size, i.e., the duration of the observations. Concomitant with this lack of convergence is the gradual increase of the correlation time or  $e$ -folding time with sample size. This correlation time, which is often interpreted as the integral scale, keeps on increasing. In the slow solar wind, for example, its value starts at 0.7 hr for intervals of 10 hr and exceeds 7 hr when intervals of 300 hr are taken; these are about the longest intervals we can reasonably observe in the slow solar wind. These results already raise serious concerns about the possibility of meaningfully estimating the ACF and the integral scale from solar wind observations.

Technically speaking, the lack of convergence of the ACF refers to the consistency of the estimator and provides no proof of non-stationarity. However, we can go one step further. From the observational evidence for power laws in the PSD of the magnetic field we can derive theoretical expressions for the ACF (Equations (6)–(8)) and find that depending on the value of the spectral index  $\gamma$  the ACFs may or may not converge. Therefore, the lack of convergence we observe is not just a property of the estimator (i.e., because we are working with finite samples) but also stems from the non-stationarity of the population.

The second major result is the large variance of the ACF estimates, as illustrated in Figure 2. Such a large dispersion seriously undermines our capacity to draw meaningful physical conclusions. This effect has been chronically overlooked in the literature, probably because very few studies provide ACFs with uncertainties. Large uncertainties are not a problem per se as long as they can be reduced by considering longer time intervals. Figure 8, however, tells us that this helps only when the spectral index is sufficiently small, i.e., for  $\gamma < 1$ . For steeper spectra, typically in the inertial range, the uncertainty of the average ACF cannot be notably reduced by increasing the duration  $T$ . This effect persists for spectral indices that correspond to the sub-ion range of solar wind turbulence, for  $\gamma > 2$ . For steeper spectra, longer durations help again but the dispersion of the ACFs remains large. For example, to reduce the uncertainty of the average ACF by a factor of 10, the averaging needs to be performed over a record that is approximately  $10^2$  longer when  $\gamma < 0.5$ ,  $10^{14}$  times longer when  $\gamma = 5/3$  and  $10^5$  times longer when  $\gamma = 3$ . Clearly, these numbers are prohibitively large for spectral indices that typically exceed 0.5.

At very long timescales of weeks or more the  $f^{-1}$  scaling of the PSD should eventually break down to prevent an infrared catastrophe; the amount of energy that is injected into the solar wind cannot grow indefinitely. Such a low-frequency cutoff has not been observed experimentally. For these reasons we can only conjecture that the wind should eventually become stationary.

The picture that emerges from these results is a scale-dependent non-stationarity. The question whether the solar wind is stationary or not is ill-posed. We find strong evidence for signatures of non-stationarity in the inertial range and in the  $f^{-1}$  range. These are the frequency intervals in which the ACF suffers from a high variance and converges slowly, precluding the estimation of meaningful correlation times.

Outside of that range, stationarity may become a reasonable assumption. A similar picture can be found, for example, in terrestrial imaging (Flandrin & Borgnat 2008): land surface images look non-stationary at scales when cities and streets can

be clearly identified. At smaller scales and at larger scales they tend to look more stationary because no major features stand out.

The reason for this non-stationarity resides in the statistical properties of the ACF for a self-affine process. These properties have been well documented in the literature, (e.g., Sornette 2004). Several methods have been developed for mitigating their deleterious effects. Detrended fluctuation analysis (Peng et al. 1994; Hu et al. 2001) is a popular one; in this method polynomials of various orders are adjusted and then subtracted in place of the mean value. This method has been shown to perform well when the observations are affected by some external trend. In the case of the solar wind, low-frequency trends are intrinsically part of the wind, and so their subtraction becomes questionable.

Another key result is the impossibility of deriving meaningful characteristic scales from the ACF in the inertial and  $f^{-1}$  ranges. The inertial scale length cannot be properly inferred from the ACF because its value depends both on the underlying physics, on the duration of the time intervals, and on the number of intervals used for averaging. Taking longer intervals or increasing their number offers no remedy and merely increases the false impression that the estimator is more accurate, especially since averaged ACFs tend to be smooth functions of the lag  $\tau$ , thereby giving the false impression that they are accurate. This misleading result questions the validity of correlation times that are published in the literature.

Our results also suggest that one should avoid working in the time domain to obtain accurate measurements of characteristic times. The Fourier transform offers a valuable alternative and has indeed often been used for such purposes. However, because the Fourier transform also formally requires stationarity, it is not ideally suited for self-affine processes. The discrete wavelet transform has been shown to be more appropriate because it is self-affine by construction (Mallat 2008). In particular, wavelets provide a better (unbiased) estimator of the spectral index (Abry et al. 1995) and so should systematically be preferred to the Fourier transform.

Let us finally address Taylor’s “frozen-in” assumption, which is often used to convert temporal scales into more natural spatial ones. This assumption is known to hold well in the inertial range and in the sub-ion ranges when the advection effects are dominant over the dispersive effects (Matthaeus & Goldstein 1982a). We expect it to break down for rapidly evolving structures such as shears and rapid rotations of the magnetic field. It should also break down when the eddy size becomes comparable to the Sun–Earth distance, i.e., for timescales of several days. Such limitations have already been recognized by Perri & Balogh (2010) and suggest that the correspondence between temporal stationarity and spatial homogeneity is not automatic. To avoid any ambiguity in the interpretation of our scales, we prefer to keep on working in the time domain, and convert to spatial scales only when necessary.

## 5. Conclusion

In this study we revisit the question of weak stationarity in the solar wind through the lens of the ACF. While the ACF has not been designed to test stationarity, it is sensitive to it and its abundant use in solar wind studies motivates its study here. We observe clear signatures of non-stationarity, both in the fast and in the slow solar wind although no rigorous proof can be given.

In addition, these signatures arise in specific frequency ranges only. Therefore, the common question of whether the solar wind is stationary or not is ill-posed.

To reach these conclusions we use the observational evidence for power-law scalings in the PSD of magnetic field fluctuations measured at 1 au by the *WIND* satellite. We first reveal that for such power laws the analytical expressions of the ACFs are ill-behaved because of self-similarity. Records whose spectral index is between 1 and 2 (typically, for the inertial range, for which the spectral index is 5/3) the ACFs suffer from a high variance and converge very slowly to a stable mean value. Actually their convergence is so slow that the estimated ACFs cannot be meaningfully estimated from finite observations, even with years of data. Likewise, the correlation time that is routinely inferred from ACFs is more likely to be affected by the length of the observed sequence rather than by the physical timescales associated with the turbulent eddies. These insidious pitfalls have often been overlooked and highlight the need for more systematic validation of correlation measures.

These convergence problems persist for spectral indices greater than 2, i.e., in the sub-ion range and in the electron kinetic range of solar wind turbulence, which should therefore be considered as non-stationary. We conjecture that for very long timescales, typically of the order of several days or weeks, stationarity may set in again because in the solar wind the spectral energy content cannot grow indefinitely at low frequencies. However, as of today, these very long timescales have not yet been observed and so even records that are several days long should be treated with the utmost care.

Based on these results we recommend avoiding using the ACF as a estimator of eddy size in the inertial and  $f^{-1}$  regimes, even when the duration of the record exceeds the correlation time by a considerable amount (2 orders of magnitude and more). Working in Fourier space offers a good alternative. Even better is the wavelet transform, which is ideally suited for studying self-affine processes.

However, there is a caveat in our study. Here, we address weak stationarity only, which considers first- and second-order moments only of the wavefield. Higher-order moments are usually ignored because their assessment is increasingly difficult. These moments, however, are precisely the ones that give insight into the existence of phase couplings, which may give rise to coherent structures such as shocks, rapid rotations, or compressions. These structures are inherent to the solar wind.

Therefore, the weak stationarity we have studied does not exclude the presence of small-scale structures that may be locally organized and in this sense make the wavefield inhomogeneous in space, and non-stationary in time. The way forward to assessing the role of such structures is by means of higher-order moments, or their Fourier equivalent, which are higher-order spectra.

V.K.J. is supported by the French Space Agency (CNES) and Région Centre-Val de Loire PhD grant (CNES N° 5100016274). We would like to thank Olga Alexandrova for useful discussions and we also thank the Space Physics Data Facility (SPDF) and Adam Szabo, the Principal Investigator of the *WIND* Magnetic Field Investigation for providing the data. T.D. and V.K. acknowledge the financial support of CNES for

the accompanying science program on the Parker Solar Probe and on the Solar Orbiter.

### ORCID iDs

Vamsee Krishna Jagarlamudi  <https://orcid.org/0000-0001-6287-6479>

Thierry Dudok de Wit  <https://orcid.org/0000-0002-4401-0943>

Vladimir Krasnoselskikh  <https://orcid.org/0000-0002-6809-6219>

### References

- Abry, P., Goncalves, P., & Flandrin, P. 1995, in *Wavelets in Statistics* (Lecture Notes in Statistics Vol. 103), ed. A. Antoniadis & G. Oppenheim (Berlin: Springer), 15
- Alexandrova, O., Chen, C. H. K., Sorriso-Valvo, L., Horbury, T. S., & Bale, S. D. 2013, *SSRv*, **178**, 101
- Aschwanden, M., Crosby, N., Dimitropoulou, M., et al. 2016, *SSRv*, **198**, 47
- Bartlett, M. S. 1946, *Supplement to the Journal of the Royal Statistical Society*, **8**, 27
- Batchelor, G. K. 1953, *The Theory of Homogeneous Turbulence* (Cambridge: Cambridge Univ. Press)
- Bendat, J. S., & Piersol, A. G. 2000, *Random Data Analysis and Measurement Procedures* (New York, London: Wiley)
- Beran, J. 1994, *Statistics for Long-memory Processes* (New York: Chapman and Hall)
- Beran, J., Feng, Y., Ghosh, S., & Kulik, R. 2016, *Long-Memory Processes: Probabilistic Properties and Statistical Methods* (New York: Springer)
- Borgnat, P., & Flandrin, P. 2009, *JSMTE*, **1**, 1
- Bruno, R., & Carbone, V. 2013, *LRSP*, **2**, 4
- Dickey, D. A., & Fuller, W. A. 1979, *J. Am. Stat. Assoc.*, **74**, 427
- Flandrin, P. 1989, *ITIT*, **35**, 197
- Flandrin, P., & Borgnat, P. 2008, *Journal of Physics Conference Series*, **139**, 012004
- Franzke, C. L. E., Graves, T., Watkins, N. W., Gramacy, R. B., & Hughes, C. 2012, *RSPTA*, **370**, 1250
- Franzke, C. L. E., Osprey, S. M., Davini, P., & Watkins, N. W. 2015, *NatSR*, **5**, 9068
- Frisch, U. 1995, *Turbulence: the Legacy of A.N. Kolmogorov* (Cambridge: Cambridge Univ. Press)
- Gardner, W. A., Napolitano, A., & Paura, L. 2006, *SigPr*, **86**, 639
- Ghil, M., Allen, M. R., Dettinger, M. D., et al. 2002, *RvGeo*, **40**, 1003
- Gilmore, M., Yu, C. X., Rhodes, T. L., & Peebles, W. A. 2002, *PhPI*, **9**, 1312
- Graves, T., Gramacy, R. B., Watkins, N., & Franzke, C. 2017, *Entp*, **9**, 437
- Hooze, F. N., & Bobbert, P. A. 1997, *PhyB*, **239**, 223
- Hooze, F. N., Kleinpenning, T. G. M., & Vandamme, L. K. J. 1981, *RPPH*, **44**, 479
- Hu, K., Ivanov, P. C., Chen, Z., Carpena, P., & Eugene Stanley, H. 2001, *PhRvE*, **64**, 011114
- Isaacs, J. J., Tessein, J. A., & Matthaeus, W. H. 2015, *JGRA*, **120**, 868
- Kasdin, N. J. 1995, *IEEEP*, **83**, 802
- Keshner, M. S. 1982, *IEEEP*, **70**, 212
- King, J. H., & Papitashvili, N. E. 2005, *JGRA*, **110**, A02104
- Kiyani, K. H., Chapman, S. C., & Watkins, N. W. 2009, *PhRvE*, **79**, 036109
- Kiyani, K. H., Osman, K. T., & Chapman, S. C. 2015, *RSPTA*, **373**, 20140155
- Klein, L. W., Matthaeus, W. H., Roberts, D. A., & Goldstein, M. L. 1992, in *Solar Wind Seven*, Proc. 3rd COSPAR Coll., ed. E. Marsch & R. Schwenn (Oxford: Pergamon Press), 197
- Lepping, R. P., Acuña, M. H., Burlaga, L. F., et al. 1995, *SSRv*, **71**, 207
- Mallat, S. 2008, *A Wavelet Tour of Signal Processing: The Sparse Way* (3rd ed.; London: Academic)
- Mandelbrot, B. 1999, *Multifractals and 1/f Noise: Wild Self-Affinity in Physics* (New York: Springer)
- Marquette, M. L., Lillis, R. J., Halekas, J. S., et al. 2018, *JGRA*, **123**, 2493
- Marsch, E., & Tu, C.-Y. 1997, *NPGeo*, **4**, 101
- Matthaeus, W. H., Dasso, S., Weygand, J. M., et al. 2005, *PhRvL*, **95**, 231101
- Matthaeus, W. H., & Goldstein, M. L. 1982a, *JGR*, **87**, 6011
- Matthaeus, W. H., & Goldstein, M. L. 1982b, *JGR*, **87**, 10347
- Matthaeus, W. H., Smith, C. W., & Oughton, S. 1998, *JGRA*, **103**, 6495
- Matthaeus, W. H., Wan, M., Servidio, S., et al. 2015, *RSPTA*, **373**, 20140154
- Moloney, N. R., & Davidsen, J. 2011, *GeoRL*, **38**, L14111
- Moloney, N. R., & Davidsen, J. 2014, *PhRvE*, **89**, 052812
- Munteanu, C., Negrea, C., Echim, M., & Mursula, K. 2016, *AnGeo*, **34**, 437
- Nicol, R. M., Chapman, S. C., & Dendy, R. O. 2009, *ApJ*, **703**, 2138
- Papoulis, A., & Pillai, S. U. 2002, *Probability, Random Variables and Stochastic Processes* (4th ed.; New York: McGraw-Hill)
- Peng, C.-K., Buldyrev, S. V., Havlin, S., et al. 1994, *PhRvE*, **49**, 1685
- Perri, S., & Balogh, A. 2010, *ApJ*, **714**, 937
- Podesta, J. J., Galvin, A. B., & Farrugia, C. J. 2008, *JGRA*, **113**, A09104
- Podesta, J. J., & Roberts, D. A. 2005, in *ESA Special Publication 592, Solar Wind 11/SOHO 16, Connecting Sun and Heliosphere*, ed. B. ed. Fleck, T. H. Zurbuchen, & H. Lacoste (Noordwijk: ESA), 531
- Press, W. H., Teukolsky, S. A., Vetterling, W. T., & Flannery, B. P. 2002, *Numerical Recipes: The Art of Scientific Computing* (3rd ed.; Cambridge: Cambridge Univ. Press)
- Priestley, M. B. 1988, *Non-linear and Non-stationary Time Series* (London: Academic)
- Priestley, M. B., & Rao, T. S. 1969, *Journal of the Royal Statistical Society. Series B (Methodological)*, **31**, 140
- Richardson, J. D., & Paularena, K. I. 2001, *JGR*, **106**, 239
- Ruiz, M. E., Dasso, S., Matthaeus, W. H., & Weygand, J. M. 2014, *SoPh*, **289**, 3917
- Rust, H. W., Mestre, O., & Venema, V. K. C. 2008, *JGRD*, **113**, D19110
- Scargle, J. D. 1989, *ApJ*, **343**, 874
- Sornette, D. 2004, *Critical Phenomena in Natural Sciences: Chaos, Fractals Selforganization and Disorder: Concepts and Tools* (2nd ed.; Berlin: Springer)
- Theiler, J., Eubank, S., Longtin, A., Galdrikian, B., & Doyne Farmer, J. 1992, *PhyD*, **58**, 77
- Tu, C.-Y., & Marsch, E. 1995, *SSRv*, **73**, 1
- Veltri, P. 1999, *PPCF*, **41**, A787
- Weygand, J. M., Matthaeus, W. H., Kivelson, M. G., & Dasso, S. 2013, *JGRA*, **118**, 3995
- Wicks, R. T., Owens, M. J., & Horbury, T. S. 2010, *SoPh*, **262**, 191
- Witt, A., Kurths, J., & Pikovsky, A. 1998, *PhRvE*, **58**, 1800